64
Review paper
Doi 10.61892/STP202601099M
ISSN 2566-4484

Miloš Marković, High School of Civil Engineering and Geodesy, markovicmilos29@gmail.com
Aleksandar Savić, University of Belgrade, savic.alexandar@gmail.com
Anja Terzić, Institute for Testing of Materials IMS, anja.terzic@institutims.rs

APPLICATION OF GROUND-PENETRATING RADAR (GPR) SCANNING TECHNOLOGY IN THE INSPECTION OF CONCRETE STRUCTURES

Abstract:

In this paper, the authors address the inspection of concrete structures using ground-penetrating radar (GPR) scanning technology. The main idea is focused on the inspection of a concrete structure for the purpose of detecting reinforcement or objects with a circular cross-section. The analysis includes both dry and wet concrete, as well as metallic and non-metallic objects with a circular cross-section. The practical part of the study contains real radargrams covering a reinforced concrete slab and a reinforced concrete bridge column. In addition to real radargrams, synthetic radargrams simulating various scenarios were also analyzed. The obtained results demonstrate the wide applicability and potential of ground-penetrating radar scanning technology in this specific field of civil engineering.

Keywords: Concrete structure, scanning, reinforcement, detection, ground-penetrating radar (GPR)

ПРИМЕНА ГЕОРАДАР ТЕХНОЛОГИЈЕ СКЕНИРАЊА КОД ИНСПЕКЦИЈЕ БЕТОНСКИХ КОНСТРУКЦИЈА

Сажетак:

У овом раду аутори се баве инспекцијом бетонских конструкција применом технологије скенирања георадаром. Основна идеја огледа се у инспекцији бетонске конструкције у циљу детекције арматуре или детекцији објеката кружног попречног пресека. Анализа укључује сув и влажан бетон као и метални и неметални објекат кружног попречног пресека. Практичан део рада садржи реалне радарграме који обухватају армирану бетонску плочу и армирани бетонски стуб мостовске конструкције. Поред реалних радарграма анализирани су и синтетички радарграми који симулирају различите сценарије. Добијени резултати показују широку примену и могућности технологије скенирања георадаром и у овој специфичној области грађевинарства.

Кључне ријечи: бетонска конструкција, скенирање, арматура, детекција, георадар.

1. INTRODUCTION

Inspection of concrete plays important role in maintenance and detection of changes in structures. Compared to invasive inspection methods that are more demanding and time consuming, non-destructive methods, such as ground penetrating radar (GPR) are more suitable for application in field conditions [1]. Based on GPPR scanning results material properties can be estimated and suitable plan of remediation or other required works can be made if anomalies are detected. This provides safe and reliable function of analysed structure and its lifetime is extended. When scanning concrete structures with GPR a particular attention should be given to boundary surfaces that cause the reflection of electromagnetic waves. This includes the boundary between compacted material and some anomaly, boundaries between good-quality and degraded concrete, surface between concrete and insulation materials, as well as the transition ones between dry and wet concrete. Also, strong reflection caused by metallic parts such as bolts and fasteners must not be neglected [2]. In practice sensors are often used to determine relative humidity of the concrete [3], [4], [5]. However, relative humidity is influenced by atmospheric conditions, which makes these sensors less reliable when estimating the efficiency of concrete hardening process. Therefore other approaches are used. One of them is to measure relative dielectric constant (relative permittivity) which represents the resistance that material has to propagation of electromagnetic waves. In recent years relative dielectric constant of the concrete is more frequently used to assess the ratio between water and cement (w/c) in freshly made concrete [6], [7], as well as to estimate the water content in hardened concrete [8]. Table 1 contains typical values of relative dielectric constant of concrete components.

Table 1. Relative dielectric constant values of concrete components [2]

Materials	**Dielectric constant**
Limestone-dry	4-8
Limestone-wet	6-15
Sand-dry	3-6
Sand-wet	10-15

In this paper we analyse the radargrams obtained by GPR scanning of dry and wet concrete. The aim of the analysis is to estimate the differences when detecting rebar or cylindrical objects buried in concrete of various humidity levels. This analysis results show the applicability of GPR technology in concrete inspection and provides better interpretation of obtained results for the detection of rebar or other anomalies contained in analysed zone.

1.1. GROUND PENETRATING RADAR (GPR) TECHNOLOGY

Nowadays, GPR is one of the frequently used non-invasive detection methods [2]. The device itself is most instancees modular and is comprised of control unit, antenna and the cable connecting them. Also, other components can be added, such as incremental encoder, providing relative position, or GPS/GNSS receiver providing absolute position along the scanning path. The configuration of the device therefore can be optimized for specific application. During acquisition the transmitting antenna emits high-frequency EM waves and directs them into the object or the soil. When emitted signal reaches the surface of the concrete or the soil, one part of it reflects to receiving antenna while the other part continues propagating through the medium by refraction or dispersion. Once the reflected part of EM wave reaches the receiving antenna it is converted into digital signal and its amplitude values are written into the column of a matrix. Number of cells in a column (i.e. number of samples) is defined by the operator before the scanning and this column represents one reflected and received signal called A-scan (Fig. 1a). A number of subsequent columns represent basic scanning result called the B-scan or radargram (Fig. 1b). Essentially, B-scan is 2D matrix contain amplitudes of reflected EM wave from consequent positions along the scanning trajectory and from various depths. Also, a 3D model, consisted of several B-scans can be formed, with parallel or perpendicular scanning trajectories. Then it is possible to extract a horizontal cross-section at desired depth. This cross-section is called time-slice or C-scan (Fig. 1c). Like in the majority of analyses, inspection of concrete structures properties is based on the analysis of reflected EM waves forms.

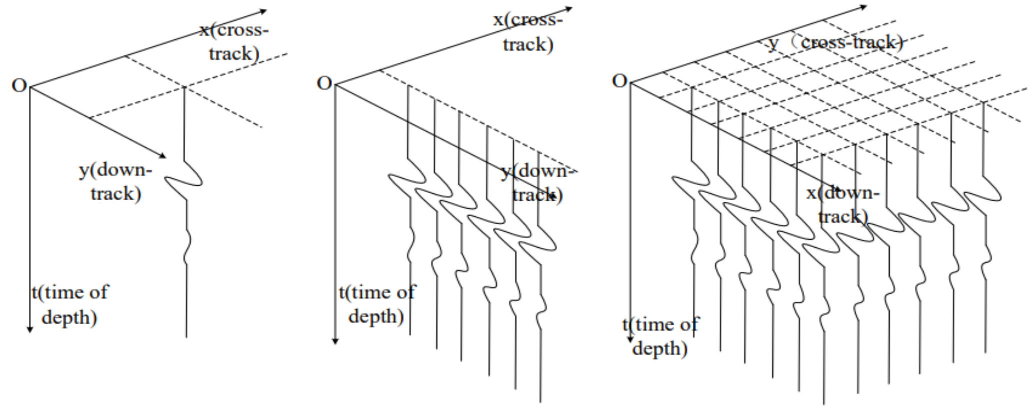

a) b) c)

Figure 1. A-scan (a), B-scan (b), and C-scan data (c) [9]

2. GPR APPPLICATIONS IN CIVIL ENGINEERING

Research in the field of GPR was intensive during last few decades and many improvements were made for applications in civil engineering. The usage of GPR in analysis and inspection of concrete structures is one of the leading non-destructive testing ways for obtaining information on inner structure. Widespread usage of GPR is primarily associated to two facts [10]: acquisition in the field is fast and efficient, with the results being available almost instantly, and the resolution of radargram can be at centimetre level, even higher, depending on the frequency range of GPR system.

In the area of civil engineering GPR is applied in precise locating of rebar, inspection of highways [11], inspection of tunnels [12], [13], bridges [14], [15] and similar infrastructure objects. In road inspection GPR application is not limited to layer thickness estimation [16], [17], but to a smaller embedded objects, as well as the assessment of the state of entire construction of the driveway [18]. In terms of applications on buildings there are three main areas:

- *a)* Identification of hidden elements and structures in order to protect cultural heritage and to control the compliance to regulations. Also, GPR can be used in cultural heritages state assessment [19], [20], where frequent usage is to determine the boundary layers between old and new parts of objects, built in different epochs [21] (Fig. 2a).
- *b)* Mapping of damage and material degradation, where GPR is used as a support in decision making on maintenance measures. Here the most frequent use of GPR is in detection of rebar grid [22] (Fig. 2b).
- *c)* Construction damage assessment after natural disasters, such as floods, earthquakes and landslides [23]. In those situations GPR is a tool used to determine if affected objects are safe for future use [21], [24] (Fig. 2c).

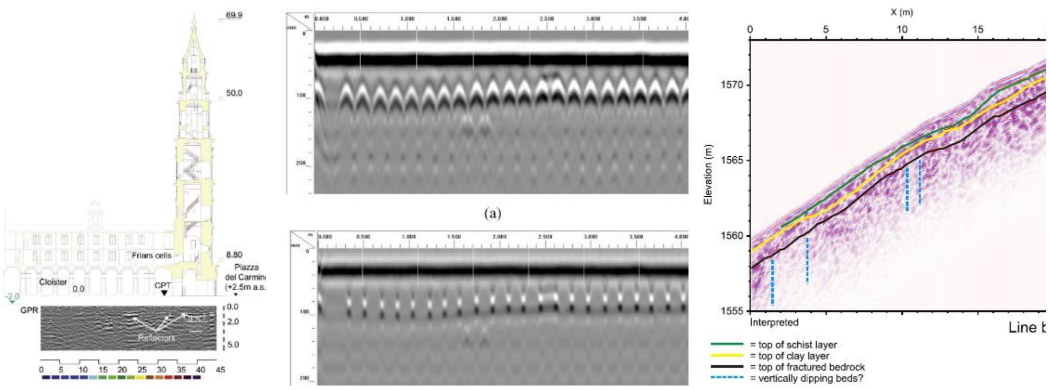

a) b) c)

Figure 2. GPR application in cultural heritage protection (a) [25], rebar grid detection (b) [22], and landslide inspection (c) [26]

3. AQUISITION

Radargram acquisition in field conditions is done on concrete pillar of bridge construction (Fig. 3) and in the underground pathway, as representative element of construction exposed to various mechanical and atmospheric influences. Both locations contain steel rebar of larger diameter and are concrete structures of high constructive and functional importance. In order to conduct more detailed inspection several parallel radargrams are collected along both axes, which provided more reliable spatial interpretation of registered reflections. Spacing between profiles is defined to provide adequate resolution of rebar detection and possible discontinuities in the concrete. Scanning is done using antenna with central frequency of 900MHz. Taking into account assumed depth and diameter of a rebar, equipment specifications are within required limits of detectability. Expected range of antenna is approximately 1.5m in dry and homogeneous concrete, while minimal diameter for detection is win the range of 1-2cm, which is adequate for standard steel rebar. Registered signals are characterized with hyperbolic reflections, typical for cylindrical objects, which enable the assessment of the position and depth of steel bars within the structure.

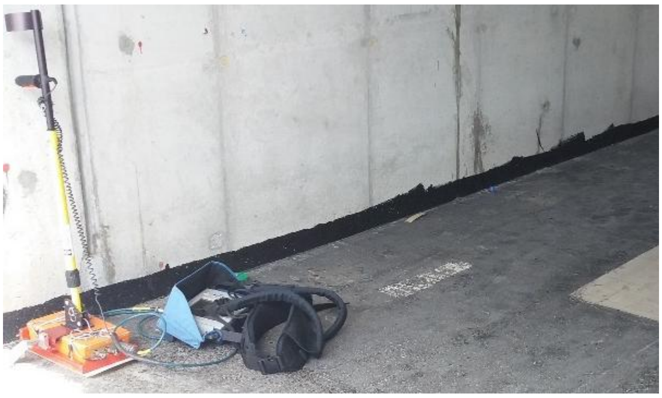

Figure 3. Scanning location and GPR equipment (photography by author).

Several synthetic radargrams are generated as well. It is done using open-source software gprMax [27]. This software provides generation of synthetic radargrams for complex scenarios. This further provides better estimation of radargrams before the field work, and for specific and complex scenarios. Many parameters can be set, such as simulation domain, material properties, soil layers, antenna models etc. As input data an *.in file has to be created, where all mentioned parameters have to be defined. In this study we assumed two values of relative dielectric constant (representing dry and wet concrete) and three different objects (steel rebar, metallic and non-metallic pipe). An example of created *in file is presented in Fig. 4.

```
#domain: 2.000 1.000 0.005
#dx_dy_dz: 0.005 0.005 0.005
#time_window: 13e-9

#material: 1 0 1 0 air
#material: 14 0 1 0 concrete

#waveform: ricker 1 0.9e9 signal
#hertzian_dipole: z 0.100 0.900 0 signal
#rx: 0.155 0.900 0
#src_steps: 0.010 0.000 0
#rx_steps: 0.010 0.000 0

#box: 0 0.900 0 2.000 1.000 0.005 air
#box: 0 0 0 2.000 0.900 0.005 concrete
#cylinder: 0.100 0.600 0 0.100 0.600 0.005 0.005 pec
#cylinder: 0.300 0.600 0 0.300 0.600 0.005 0.005 pec
#cylinder: 0.500 0.600 0 0.500 0.600 0.005 0.005 pec
#cylinder: 0.700 0.600 0 0.700 0.600 0.005 0.005 pec
#cylinder: 0.900 0.600 0 0.900 0.600 0.005 0.005 pec
#cylinder: 1.100 0.600 0 1.100 0.600 0.005 0.005 pec
#cylinder: 1.300 0.600 0 1.300 0.600 0.005 0.005 pec
#cylinder: 1.500 0.600 0 1.500 0.600 0.005 0.005 pec
#cylinder: 1.700 0.600 0 1.700 0.600 0.005 0.005 pec
#cylinder: 1.900 0.600 0 1.900 0.600 0.005 0.005 pec
```

Figure 4. Input file for GPR scanning simulation in gprMax (created by author).

4. RESULTS

4.1. SYNTHETIC RADARGRAMS

The first scenario is represented with synthetic radargrams is steel bars in concrete. In both radargrams bars diameter is 10mm, separated by 20cm and at 30cm below the surface of the concrete. In first simulation (Fig. 5a) concrete is dry with relative dielectric constant ε_r=7, while in second simulation (Fig 5b) the concrete is wet with relative dielectric constant ε_r=14. Used signal is Ricker wavelet, with central frequency f=900MHz, and the distance between consecutive scans is 1cm.In both radargrams the steel bars are clearly visible and distance between them is accurately represented. However, two differences can be noticed: bars appear to be at smaller depth in the first radargram, and reflections in second radargram are of higher intensity. To understand the first difference it has to be taken into account that the vertical axis represents the time, not the distance. Due to lower relative dielectric constant of dry concrete the propagation velocity of EM waves is higher and it takes less time for the wave to travel from transmitting antenna, to reflector, and then back to receiving antenna. Therefore, even though the bars appear to be at smaller depth in dry concrete, one has to take into account the concrete properties when estimating depth. Higher intensity of reflections in second radargram are not expected since the higher relative constant of the concrete is not only causing the lower propagation velocity but higher attenuation as well. However, the reflection amplitude, i.e. visible intensity of the reflection depends on the difference between two meeting materials rather than on dielectric constant of the concrete alone. Taking that into account it is clear why reflection intensity in second radargram is higher, and, in general, it shows that detection of metallic objects is easier in wet than in dry concrete, even though the maximum penetration depth of EM waves is lower.

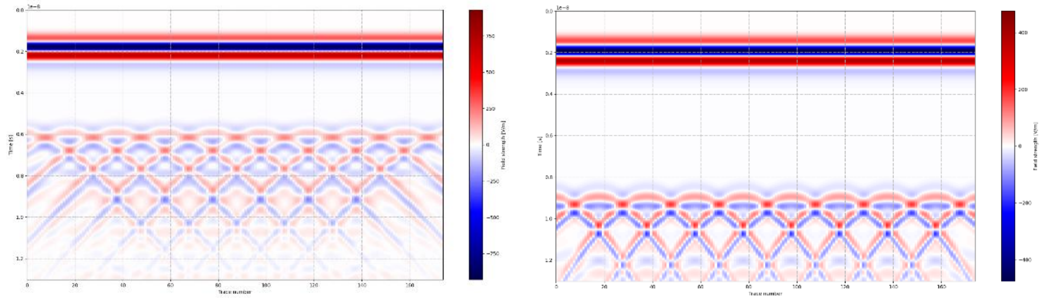

a) b)

Figure 5. Synthetic radargrams of steel rebar in dry (a) and wet concrete (b)(created by author).

The second scenario involves two pipes of the same diameter, one metallic and one non-metallic in concrete (Fig. 6). In both radargrams the diameter of the pipes is the same (mm) and they are at the same depth (30cm below the surface of the concrete). First pipe is metallic while the material of the second one is PVC and it is hollow (that is, filled with air or some other gas). As in the first scenario relative dielectric constants of the concrete are 7 and 14, respectively.

Two differences, noticeable in first scenario, are visible here as well. Reflections appear at bigger depth and with increased intensity. The interpretation of these differences is the same as in first scenario. However, one more difference can be noticed here. Hyperbolic reflections appear to be wider in dry than in wet concrete which can suggest that pipes in Fig. 6a are of bigger diameter than the ones in Fig. 6b.

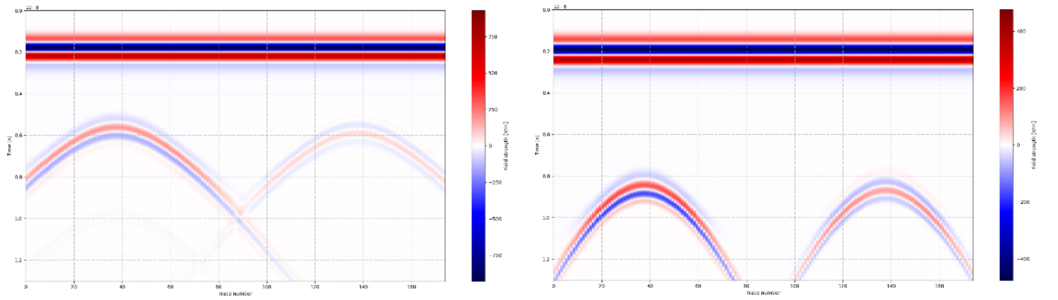

a) b)

Figure 6. Synthetic radargrams of metallic and non-metallic cylindrical object in dry (a) and wet concrete (b) (created by author).

This is also the consequence of lower relative dielectric constant of dry concrete ant thus higher propagation velocity. Reflected waves that arrive to receiving antenna at oblique angles take less time to reach the antenna in case of dry concrete and it results in wider hyperbolic shape. This difference is present in radargrams in Fig 5 as well, but due to smaller dimension of the reflectors and theirs hyperbolic reflection it is less noticeable.

4.2. REAL RADARGRAMS

Real radargrams created by scanning concrete pillar with steel rebar contain hyperbolic reflections at approximately 30cm of depth (Fig. 7). Spacing between bars is around 30cm. As in synthetic radargrams radargram created on dry concrete appears to have lower amplitudes than the one created on wet concrete. Also, in both radargrams the surface layer (up to 25cm deep) contains pixels with lower amplitudes, which suggests that water content is very low. Unlike in synthetic radargram, rebar appears to be at the same depth in both real radargrams. This is the consequence of vertical scale units. Here vertical axis represents distance (i.e. depth), while in synthetic radargrams it represented time.

Hyperbolic reflections in these radargrams are much less noticeable than in synthetic radargrams. They also show less details and, even though they are made using the same central frequency (900MHz) images visibly appear to be in lower resolution. These are the consequence of real scanning conditions and technology limitations (noisy environment, real characteristics of equipment, minor imprecisions by the operator, etc.) that simply don't exist when running simulation and generating idealistic, synthetic radargrams. However, as represented, still many information can be extracted from real radargrams: horizontal and vertical position of rebar, spacing between bars, estimation of water content in the concrete, etc. Using antenna of higher central frequency and refining the acquisition procedure can only improve obtained results and provide more accurate information.

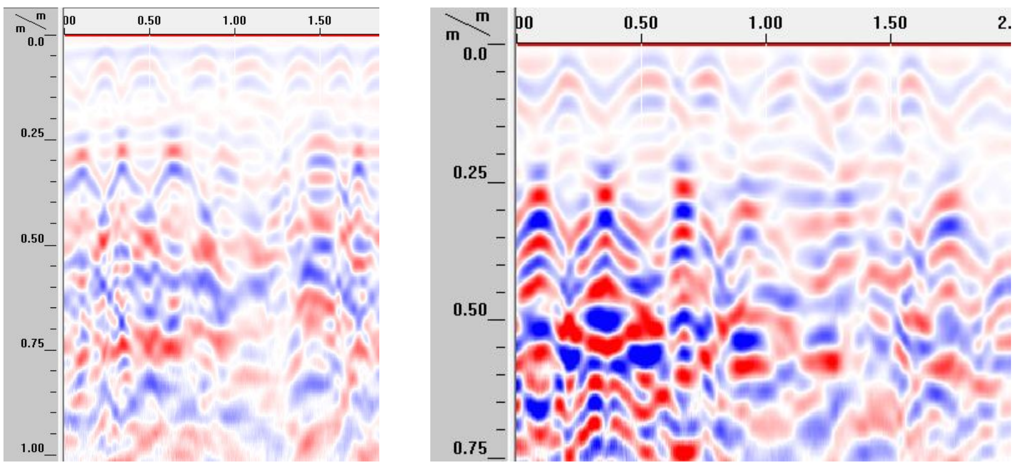

a) b)

Figure 7. Real radargrams with rebar reflections in dry (a) and wet concrete (b) (created by author).

5. CONCLUSION

In this paper an analysis of GPR technology application for concrete structures inspection was conducted, with emphasis on capabilities for rebar grid detection and the assessment of influence of moisture content to the quality of obtained results. As the case study, a concrete pillar of a bridge is analysed. Also, several synthetic radargrams are generated in order to compare expected and obtained results and to provide more accurate interpretation. Combining real and numerically simulated data provided more reliable recognition of hyperbolic reflection that indicate the presence of rebar in the concrete. Analysis results confirm that 900MHz antenna usage can be successfully used to detect rebar, as well as other anomalies in concrete structures, achieving satisfying compromise between penetration depth of EM waves and resolution. Also, the analysis of moisture content indicated that GPR technology can be successfully used to assess the moisture distribution within the concrete structures. Although there are noticeable differences between real and synthetic radargrams, this analysis shows that GPR can be considered as an efficient, quick and reliable non-destructive method for inspection of concrete structures, especially in the area of state assessment and remediation planning.

ACKNOWLEDGMENT

This research has been supported by the Ministry of Science, Technological Development and Innovation (Contract No. 451-03-34/2026-03/200156) and the Faculty of Technical Sciences, University of Novi Sad through project “Scientific and Artistic Research Work of Researchers in Teaching and Associate Positions at the Faculty of Technical Sciences, University of Novi Sad 2026” (No. 01-3609/1).

LITERATURE

[1] R. He, T. Nantung, J. Olek, and N. Lu, "Field study of the dielectric constant of concrete: A parameter less sensitive to environmental variations than electrical resistivity," *J. Build. Eng.*, vol. 74, 2023, Art. no. 106938, https://doi.org/10.1016/j.jobe.2023.106938

[2] H. M. Jol, *Ground Penetrating Radar Theory and Applications*. 1st ed. Amsterdam, The Netherlands: Elsevier, 2009., ISBN:978-0-444-53348-7

[3] P. Sun, "A new protocol for evaluating concrete curing effectiveness," *Ph.D. dissertation, Texas A&M Univ*., College Station, TX, USA, 2013., https://hdl.handle.net/1969.1/151295

[4] A. Joshaghani and D. G. Zollinger, "Concrete pavements curing evaluation with non destructive tests," *Constr. Build. Mater*., vol. 154, pp. 1250–1262, 2017., https://doi.org/10.1016/j.conbuildmat.2017.06.110

[5] J.-H. Jeong and D. G. Zollinger, "Development of test methodology and model for evaluation of curing effectiveness in concrete pavement construction," *Transp. Res. Rec*., vol. 1861, pp. 17–25, 2003., https://doi.org/10.3141/1861-03

[6] R. He, T. Nantung, J. Olek, and N. Lu, "Use of dielectric constant for determination of water-to-cement ratio (W/C) in plastic concrete: Part 1. Volumetric water content modeling," *ES Mater. Manuf*., 2023. https://doi.org/10.30919/esmm5f866

[7] R. He, T. Nantung, J. Olek, and N. Lu, "Use of dielectric constant for determination of water to-cement ratio (W/C) in plastic concrete: Part 2: Comparison of determined W/C values by ground penetrating radar (GPR) and microwave oven drying measurements," *ES Mater. Manuf.*, 2023., https://doi.org/10.30919/esmm5f874

[8] G. Leucci, "Ground penetrating radar: An application to estimate volumetric water content and reinforced bar diameter in concrete structures," *J. Adv. Concr. Technol*., vol. 10, pp. 411–422, 2012, https://doi.org/10.3151/jact.10.411

[9] X. Bai, Y. Yang, S. Wei, G. Chen, H. Li, Y. Li, and H. Cui, "A comprehensive review of conventional and deep learning approaches for ground-penetrating radar detection of raw data," *Appl. Sci*., vol. 13, no. 13, 2023, Art. no. 7992, https://doi.org/10.3390/app13137992

[10] W. W. L. Lai, X. Derobert, and P. Annan, "A review of ground penetrating radar application in civil engineering: A 30-year journey from locating and testing to imaging and diagnosis," *NDT E Int*., vol. 96, pp. 58–78, 2018, https://doi.org/10.1016/j.ndteint.2017.04.002

[11] Z. Liu, B. Cui, and X. Gu, "TIGPR: A multi-view ground penetrating radar detection data for damage assessment of transportation infrastructure," *Data Brief*, vol. 60, 2025, Art. no. 111665, https://doi.org/10.1016/j.dib.2025.111665

[12] Q.-M. Yu, H.-L. Zhou, Y.-H. Wang, and R.-X. Duan, "Quality monitoring of metro grouting behind segment using ground penetrating radar," *Constr. Build. Mater*., vol. 110, pp. 189–200, 2016., https://doi.org/10.1016/j.conbuildmat.2015.12.109

[13] A. Lalagüe, M. A. Lebens, I. Hoff, and E. Grøv, "Detection of rockfall on a tunnel concrete lining with ground-penetrating radar (GPR)," *Rock Mech. Rock Eng*., vol. 49, pp. 2811–2823, 2016.

[14] M. I. Hasan and N. Yazdani, "Ground penetrating radar utilization in exploring inadequate concrete covers in a new bridge deck," *Case Stud. Constr. Mater*., vol. 1, pp. 104–114, 2014., https://doi.org/10.1016/j.cscm.2014.04.003

[15] A. V. Varnavina, A. K. Khamzin, L. H. Sneed, E. V. Torgashov, N. L. Anderson, and N. H. Maerz, "Concrete bridge deck assessment: Relationship between GPR data and concrete removal depth measurements collected after hydrodemolition," *Constr. Build. Mater*., vol. 99, pp. 26–38, 2015., https://doi.org/10.1016/j.conbuildmat.2015.09.008

[16] M. Varela-González, M. Solla, J. Martínez-Sánchez, and P. Arias, "A semi-automatic processing and visualisation tool for ground-penetrating radar pavement thickness data," *Autom. Constr*., vol. 45, pp. 42–49, 2014, https://doi.org/10.1016/j.autcon.2014.05.004

[17] S. Zhao, P. Shangguan, and I. L. Al-Qadi, "Application of regularized deconvolution technique for predicting pavement thin layer thicknesses from ground penetrating radar data," *NDT E Int*., vol. 73, pp. 1–7, 2015., https://doi.org/10.1016/j.ndteint.2015.03.001

[18] M. Sun, C. Le Bastard, N. Pinel, Y. Wang, J. Li, and J. Pan, "Estimation of time delay and interface roughness by GPR using modified MUSIC," *Signal Process*., vol. 132, pp. 272–283, 2017, https://doi.org/10.1016/j.sigpro.2016.05.029

[19] S. Hemeda, Ground Penetrating Radar (GPR) Investigations for Architectural Heritage Preservation: The Case of Habib Sakakini Palace. Cairo, Egypt, 2012.

[20] V. Pérez-Gracia, J. Caselles, J. Clapés, G. Martinez, and R. Osorio, "Non-destructive analysis in cultural heritage buildings: Evaluating the Mallorca cathedral supporting structures," *NDT E Int*., vol. 59, pp. 40–47, 2013, https://doi.org/10.1016/j.ndteint.2013.04.014

[21] F. García García, M. Ramírez Blanco, I. Rodríguez Abad, R. Martínez Sala, I. Tort Ausina, and J. Benlloch Marco, "GPR technique as a tool for cultural heritage restoration: San Miguel de los Reyes Hieronymite Monastery, 16th century (Valencia, Spain)," *J. Cult. Herit.*, vol. 8, pp. 87–92, 2007, https://doi.org/10.1016/j.culher.2006.10.005

[22] K. Dinh, N. Gucunski, and T. H. Duong, "Migration-based automated rebar picking for condition assessment of concrete bridge decks with ground penetrating radar," *NDT E Int*., vol. 98, pp. 45–54, 2018, https://doi.org/10.1016/j.ndteint.2018.04.009

[23] A. Ristic, B. Abolmasov, M. Govedarica, D. Petrovački, and A. Ristić, "Shallow-landslide spatial structure interpretation using a multi-geophysical approach," *Acta Geotechnica Slovenica*, 2012.

[24] C.-W. Chang, C.-H. Lin, and H.-S. Lien, "Measurement radius of reinforcing steel bar in concrete using digital image GPR," *Constr. Build. Mater*., vol. 23, pp. 1057–1063, 2009, https://doi.org/10.1016/j.conbuildmat.2008.05.018

[25] L. Evangelista, F. de Silva, A. d'Onofrio, V. Di Fiore, F. Silvestri, A. S. di Santolo, and D. Tarallo, "Application of ERT and GPR geophysical testing to the subsoil characterization of cultural heritage sites in Napoli (Italy)," *Measurement*, vol. 104, pp. 326–335, 2017, https://doi.org/10.1016/j.measurement.2016.07.042

[26] S. Carpentier, M. Konz, R. Fischer, G. Anagnostopoulos, K. Meusburger, and K. Schoeck, "Geophysical imaging of shallow subsurface topography and its implication for shallow landslide susceptibility in the Urseren Valley, Switzerland," *J. Appl. Geophys*., vol. 83, pp. 46–56, 2012, https://doi.org/10.1016/j.jappgeo.2012.05.001

[27] C. Warren, A. Giannopoulos, and I. Giannakis, "gprMax: Open source software to simulate electromagnetic wave propagation for ground penetrating radar," *Comput. Phys. Commun*., vol. 209, pp. 163–170, 2016, https://doi.org/10.1016/j.cpc.2016.08.020